

Electronic Supporting Information Available

High-performance near-infrared (NIR) polymer light-emitting diodes (PLEDs) based on bipolar Ir(III)-complex-grafted polymers

Wentao Li,^{†,‡,a} Baowen Wang,^{†,‡,a} Tiezheng Miao,^a Jiaxiang Liu,^a Guorui Fu,^{a,c,*} Xingqiang Lü^{a,*}, Weixu Feng^{b,*} and Wai-Yeung Wong^{c,*}

Supporting information

High performance liquid chromatography (HPLC)-grade THF was purchased from Fisher Scientific and purified over solvent columns. Other solvents were used as received from Sigma Aldrich and stored over 3 Å activated molecule sieves. Azobis(isobutyronitrile) (AIBN) was purified by re-crystallization twice from absolute MeOH prior to use. Other chemicals included NVK (*N*-vinyl-carbazole) and were commercial products of reagent grade and were used without further purification. All manipulations of air- and moisture-sensitive compounds were carried out under a dry N₂ atmosphere using the standard Schlenk line technique.

Elemental analyses were performed on a Perkin-Elmer 240C elemental analyzer. Fourier Transform Infrared (FT-IR) spectra were recorded on a Nicolet Magna-IR 550 spectrophotometer in the region 4000-400 cm⁻¹ using KBr pellets. ¹H NMR spectra were recorded on a JEOL EX 400 spectrometer with SiMe₄ as internal standard in CDCl₃ or DMSO-*d*₆ at room temperature. ESI-MS (was performed on a Finnigan LCQ^{DECA} XP HPLC-MS_n mass

spectrometer with a mass to charge (m/z) range of 4000 using a standard electro-spray ion source and CH_2Cl_2 as the solvent. Diffuse reflection (DR) and electronic absorption spectra in the UV/visible/NIR region were recorded with a Cary 300 UV spectrophotometer. Visible emission and excitation spectra were collected by a combined fluorescence lifetime and steady-state spectrometer (FLS-980, Edinburgh) with a 450 W Xe lamp. Excited-state decay times were obtained by the same spectrometer but with a μF900 Xe lamp. The luminescent quantum yield (Φ_{em}) in solution was measured with free-base tetraphenylporphyrin ($\Phi_r = 0.13$ in toluene solution at 298 K) as the standard.¹ The solutions were degassed by three freeze-pump-thaw circles. The following equation was used to calculate quantum yields:

$$\Phi_s = \Phi_r \cdot [(n_s^2 \cdot A_r \cdot I_s) / (n_r^2 \cdot A_s \cdot I_r)]$$

Where Φ_s is the quantum yield of the sample, Φ_r is the quantum yield of the reference, n_s is the refractive index of the sample, n_r is the refractive index of the reference, A_s and A_r are the absorbances of the sample and the reference at the wavelength of excitation (500 nm), and the I_s and I_r are the integrated areas of emission bands of the sample and the reference from 600 to 900 nm, which were recorded by a red photomultiplier tube (PMT) detector. Gel permeation chromatography (GPC) analyses of polymers were performed using a Waters 1525 binary pump coupled to a Waters 2414 refractive index detector with HPLC THF as the eluant on America Polymer Standard linear mixed bed packing columns (particle size, 10 μm). GPC was calibrated using polystyrene standards. X-ray photoelectron spectroscopy (XPS) was carried out on a PHI 5700 XPS system equipped with a dual Mg X-ray source and monochromatic Al X-ray source complete with depth profile and angle-resolved capabilities. Powder X-ray diffraction (PXRD) patterns were recorded on a D/Max-III A

diffractometer with graphite-monochromatized Cu K α radiation ($\lambda = 1.5418 \text{ \AA}$). Thermal properties were characterized using thermogravimetric (TG) and differential scanning calorimetric (DSC) analyses on a NETZSCH TG 209 instrument under flowing nitrogen at a heating rate of 10 °C/min.

Synthesis of the C^N1 main ligand Hiqbt (Hiqbt = 1-(benzo[*b*]-thiophen-2-yl)-isoquinoline)

The C^N1 main ligand **Hiqbt** was synthesized from the improved Suzuki coupling reaction² of 2-Cl-isoquinoline while not 2-Br-isoquinoline³ with benzo[*b*]thien-2-yl boronic acid. A mixture of 2-Cl-isoquinoline (0.653 g, 4.0 mmol), benzo[*b*]thien-2-yl boronic acid (0.713 g, 4.0 mmol) was dissolved into absolute mixed solvents of toluene-EtOH (60 mL; v/v = 2:1) under an N₂ atmosphere. Then an aqueous solution (20 mL) of Na₂CO₃ (2 M) was added, and the mixture was degassed by an N₂ flow. Anhydrous Pd(PPh₃)₄ (190 mg, 0.2 mmol; 5 mol%) was added to the reaction mixture and then heated at 85 °C for 48 h. The complete consumption of reagents was monitored by TLC (Hexane/AcOEt, v/v = 9:1). After cooling to RT, the organic phase was washed with brine and extracted with absolute CH₂Cl₂ (3 × 20 mL) three times. The combined organic phase was dried over anhydride Na₂SO₄, and further purified with flash-column chromatography on silica gel (Hexane/AcOEt, v/v = 9:1), affording to an off-white solid. Yield: 0.762 g (73%). Calc. for C₁₇H₁₁NS: C, 78.13; H, 4.24; N, 5.36%. Found: C, 78.05; H, 4.36; N, 5.29%. IR (KBr, cm⁻¹): 3053 (w), 2924 (w), 2361 (w), 2344 (w), 1614 (w), 1578 (w), 1549 (m), 1526 (w), 1497 (w), 1458 (w), 1437 (w), 1373 (w), 1350 (m), 1331 (w), 1252 (w), 1184 (w), 1155 (m), 1094 (w), 1070 (w), 1018 (m), 934 (m), 880 (w), 868 (w), 841 (m), 822 (s), 799 (m), 760 (s), 750 (vs), 727 (s), 698 (m), 671 (s), 654 (m), 592 (s), 555 (w), 525

(w). ^1H NMR (CDCl_3 , 400 MHz): δ (ppm) 8.61 (d, 2H, -Py), 7.95 (m, 3H, -Ph), 7.84 (s, 1H, -Th), 7.73 (t, 1H, -Ph), 7.65 (m, 2H, -Ph), 7.41 (m, 2H, -Ph).

Synthesis of the μ -chloro-bridged dimer intermediate $[\text{Ir}(\text{iqbt})_2(\mu\text{-Cl})]_2$

The μ -chloro-bridged dimer intermediate $[\text{Ir}(\text{iqbt})_2(\mu\text{-Cl})]_2$ was synthesized according to an improved Nonoyama procedure⁴ and used directly for the next step without further purification. To a mixed solvents of 2-ethoxyethanol and D. I. water (v/v = 3:1, 24 mL), **Hqbt** (400 mg, 2.6 mmol) and $\text{IrCl}_3 \cdot 3\text{H}_2\text{O}$ (208 mg, 1.2 mmol) were added, and the resultant mixture was heated overnight at 110 °C under a N_2 atmosphere. After cooling to RT, a saturate aqueous solution of NaCl (25 mL) was added and the dark-brown suspension was filtered. The brown solid products were further washed with D. I. water, diethyl ether and hexane, and dried at 45 °C under vacuum to constant weight. Yield: 82%.

Synthesis of the vinyl-functionalized $\text{C}^{\wedge}\text{N}^2$ ancillary ligand **vb-Hppy (**vb-Hppy** = 2-(4'-vinylbiphenyl-4-yl)pyridine)**

The $\text{C}^{\wedge}\text{N}^2$ -ancillary ligand **vb-Hppy** was synthesized from the improved Suzuki coupling reaction.⁵ A mixture of 4-vinylphenylboronic acid (118.4 mg, 0.8 mmol), 2-(4-bromophenyl)pyridine (198.9 mg, 0.85 mmol) was dissolved into absolute THF (20 mL) under an N_2 atmosphere. Then an aqueous solution of K_2CO_3 (2 M) was added, and the mixture was degassed by an N_2 flow. Anhydrous $\text{Pd}(\text{PPh}_3)_4$ (190 mg, 0.2 mmol; 5 mol%) was added to the reaction mixture and then heated at 80 °C for 36 h. After cooling to RT, the organic phase was extracted with $\text{CH}_2\text{Cl}_2/\text{H}_2\text{O}$ three times. The combined organic phase was dried over

anhydride Na_2SO_4 , and further purified with flash-column chromatography on silica gel (Hexane/dichloromethane, v/v = 2:3), affording to yellowish-white solid and then re-crystallized from acetone. Yield: 0.183 g (89%). Calc. for $\text{C}_{19}\text{H}_{15}\text{N}$: C, 88.68; H, 5.88; N, 5.44%. Found: C, 88.73; H, 5.83; N, 5.39%. FT-IR (KBr, cm^{-1}): 3084 (w), 3049 (w), 3001 (w), 2359 (w), 1626 (w), 1605 (w), 1584 (m), 1564 (w), 1541 (w), 1508 (w), 1497 (w), 1462 (m), 1435 (m), 1422 (w), 1398 (w), 1362 (w), 1341 (w), 1331 (w), 1298 (w), 1277 (w), 1260 (w), 1223 (w), 1188 (w), 1155 (w), 1138 (w), 1094 (w), 1059 (w), 1040 (w), 991 (m), 897 (m), 829 (s), 777 (vs), 746 (s), 691 (w), 617 (w), 584 (w), 534 (w). ^1H NMR (CDCl_3 , 400 MHz): δ (ppm): 8.70 (d, 1H, -Py), 8.08 (d, 2H, -Ph), 7.78 (d, 2H, -Ph), 7.72 (d, 2H, -Ph), 7.63 (d, 2H, -Ph), 7.51 (d, 3H, -Py), 6.78 (q, 1H, -CH=), 5.82 (d, 1H, =CH₂), 5.30 (d, 1H, =CH₂).

Synthesis of the organic precursor Br-PBD (Br-PBD = 2-(4-bromophenyl)-5-(4-tert-butylphenyl)-1,3,4-oxadiazole)

As the procedure from the literature,⁶ to a two-necked flask equipped with a stopcock and a condenser were added 4-tert-butylbenzohydrazide (231 mg, 1.2 mmol) and 4-bromobenzoic acid (200 mg, 1 mmol) under a N_2 atmosphere, with a certain amount of phosphorous oxychloride (2.5 mmol) and TEA (3.0 mmol) in EtOAc solution. After stirred at 80 °C for 24 h and cooled down to room temperature, excess phosphorous oxychloride was removed under vacuum. D. I. Water was added to the residue, and the precipitate was filtered and washed with D. I. water. The white crude product was obtained by re-crystallization from ethanol. Yield: 180 mg (90%). Calc. for $\text{C}_{18}\text{H}_{17}\text{N}_2\text{OBr}$: C, 60.52; H, 4.80; N, 7.84%. Found: C, 60.42; H, 4.93; N, 7.80%. ^1H NMR (400 MHz, $\text{DMSO}-d_6$): δ (ppm) 7.87 (m, 4 H, -Ph), 7.71 (d, 2

H, -Ph), 7.54 (d, 2 H, -Ph), 1.31 (t, 9 H, -CH₃). ESI-MS (in CH₂Cl₂) *m/z*: 357.06 (100%), [M-H]⁺.

Synthesis of the vinyl-functionalized organic monomer vinyl-PBD (vinyl-PBD = 2-(4-(*tert*-butyl)phenyl)-5-(4'-vinyl-[1,1'-biphenyl]-4-yl)-2,5-dihydro-1,3,4-oxadiazole)

According to an improved procedure from the literature,⁷ to a two-necked flask equipped with a condenser were added 2-(4-bromophenyl)-5-(4-*t*-butylphenyl)-1,3,4-oxadiazole (357.24 mg, 1.0 mmol), 4-vinylphenylboronic acid (221.94 mg, 1.5 mmol), Pd(PPh₃)₄ (0), (212.84 mg, 2 mmol) and dry toluene (25.0 mL) under nitrogen. After the solution of potassium carbonate (120 mg, 2 mmol) in oxygen-free water (2 mL) was added, the mixture was stirred at 110°C for 48 h. The resulting mixture was extracted with chloroform, and the organic layer was dried with magnesium sulfate and concentrated by rotary evaporator. The crude product was purified by silica gel column chromatography eluted with chloroform/ethyl acetate (95/5; v/v) followed by re-crystallization from methanol to yield the white crystal. Yield: 128.6 mg (36%). Calc. for C₂₆H₂₄N₂O: C, 82.07; H, 6.36; N, 7.36%. Found: C, 82.02; H, 6.41; N, 7.31%. ¹H NMR (400 MHz, DMSO-*d*₆): δ (ppm) 8.01 (d, 2 H, -Ph), 7.87 (t, 4 H, -Ph), 7.76 (d, 2H, -Ph), 7.62 (m, 2 H, -Ph), 7.54 (m, 2 H, -Ph), 6.81 (m, 1 H, -CH=), 5.93 (d, 1 H, =CH₂), 5.33 (d, 1 H, =CH₂), 1.32 (s, 9 H, -CH₃). ESI-MS (in CH₂Cl₂) *m/z*: 381.20 (100%), [M-H]⁺.

Synthesis of the AIBN-Initiated PVK (PVK = Poly(*N*-vinyl-carbazole)

The homogeneous polymerization of in activation with AIBN for comparison was carried out in a Fisher-Porter glass reactor and protected by nitrogen according to the typical procedure.

To a solution of *N*-vinyl-carbazole (NVK, 3.67 g, 19 mmol) in dry 1,2-dichlorobenzene (15 mL), AIBN initiator (46.8 mg, 1.5 mol% of NVK) was added, and the resultant homogeneous solution was purged with N₂ for 10 min and sealed under a reduced N₂ atmosphere. The mixture was heated to 80 °C with continuous stirring for 48 h. The viscous mixture was diluted with dry 1,2-dichlorobenzene (15 mL) and precipitated with absolute diethyl ether (50 mL) three times. The resulting solid PVK was collected by filtration and dried at 45 °C under vacuum to constant weight. For the **PVK**: Yield: 3.21 g (90%). FT-IR (KBr, cm⁻¹): 3074 (w), 3022 (w), 2969 (w), 2927 (w), 1623 (w), 1481 (m), 1450 (vs), 1406 (w), 1321 (s), 1220 (m), 1154 (m), 1124 (w), 1092 (w), 1031 (w), 1001 (w), 924 (w), 744 (s), 719 (s), 656 (w), 614 (w), 572 (w), 476 (w). ¹H NMR (400 MHz, DMSO-*d*₆): δ (ppm) 8.25-3.95 (b, 8H), 3.95-2.15 (b, 1H), 2.15-0.5 (b, 2H). GPC result: $M_n = 21063$ g/mol; PDI = $M_w/M_n = 1.32$.

Synthesis and characterization of the other Ir³⁺-polymers Poly(NVK-co-[Ir(iqbt)₂(vb-ppy)]) (100 or 200:1)

A mixture of NVK and complex monomers **[Ir(iqbt)₂(vb-ppy)]** at a stipulated feed molar ratio (100:1 or 200:1) in the presence of AIBN (1.5 mol-% of the monomer NVK) was dissolved in toluene (30 mL), and the resultant homogeneous solution was purged with N₂ for 10 min and sealed under a reduced N₂ atmosphere. The mixture was heated to 80 °C with continuous stirring for 48 h. The viscous mixture was diluted with toluene (15 mL) and precipitated with *n*-hexane (50 mL) three times. The resulting solid products were collected by filtration and dried at 45 °C under vacuum to constant weight, respectively. For the **Poly(NVK-co-Ir(iqbt)₂(vb-ppy))** (100:1): Yield: 93%. FT-IR (KBr, cm⁻¹): 3057 (w), 2970 (w), 2932 (w), 2359 (w), 1597 (w), 1508 (w), 1483

(m), 1450 (s), 1325 (m), 1223 (m), 1157 (w), 1124 (w), 1028 (w), 1003 (w), 926 (w), 831 (w), 745 (vs), 721 (s), 617 (w), 569 (w), 528 (w).

For the **Poly(NVK-co-Ir(iqbt)₂(vb-ppy))** (200:1): Yield: 94%. FT-IR (KBr, cm⁻¹): 3049 (w), 2967 (w), 2932 (w), 2359 (w), 1597 (w), 1508 (w), 1483 (m), 1450 (s), 1323 (m), 1223 (m), 1157 (w), 1124 (w), 1026 (w), 1002 (w), 924 (w), 831 (w), 743 (s), 719 (vs), 615 (w), 569 (w), 528 (w).

Electronic structure calculations

Theoretical studies on the electronic structure for the complex monomer **[Ir(iqbt)₂(vb-ppy)]** were carried out using density functional theory (DFT) and time-dependent DFT (TD-DFT) methods. The molecular structure was optimized at the ground state (S_0) in the gas phase. DFT calculations were conducted with the popular B3LYP functional theory. The 6-31G(d,p) basis set was applied for C, H, N, O, atoms, while effective core potentials employed for Zn atom were based on a LanL2DZ basis set.⁸⁻⁹ The excited states' energies were computed by TD-DFT based on the ground-state (S_0) geometry. Additionally, the natural transition orbital (NTO) was analyzed for $S_0 \rightarrow T_1$ excitation based on the first triplet state (T_1) geometry optimized by UB3LYP. The contributions of fragments to the "holes" and "electrons" and Inter Fragment Charge Transfer (IFCT)¹⁰ in the electronic excitation process were analyzed by the Ros and Schuit method¹¹ (C-squared population analysis method, SCPA) in the Multiwfn 3.7 program.¹² All calculations were carried out with Gaussian 09, Revision D.01 software package.¹³ The electron density diagrams of molecular orbitals were obtained with the ChemOffice 2010 graphics program.

Electrochemical determination

Cyclic voltammetry (CV) measurement was performed on a computer-controlled EG&G Potentiostat/Galvanostat model 283 at RT with a conventional three-electrode cell using an Ag/AgNO₃ (0.1 M) reference electrode, Pt carbon working electrode of 2 mm in diameter, and a platinum wire counter electrode. The CV of the sample was performed in nitrogen-saturated dichloromethane containing 0.1 M Bu₄NPF₆ as supporting electrolyte. The CV was measured at a scan rate of 100 mV·s⁻¹. The HOMO and the LUMO energy levels of each sample are calculated according to the following equations,¹⁴ $E_{\text{HOMO}} = -(E_{\text{OX}}^{\text{on}} + 4.8)$ eV, $E_{\text{LUMO}} = -(E_{\text{red}}^{\text{on}} + 4.8)$ eV, and where $E_{\text{OX}}^{\text{on}}$ is the recorded onset oxidation potential of the material, and $E_{\text{red}}^{\text{on}}$ is the recorded onset reduction potential of the material. The HOMO and LUMO energy levels for the other used materials were obtained from the literature.¹⁵

Device fabrication of the doping-type NIR-PLED-I based on the Ir³⁺-complex monomer and the grafting-type NIR-PLEDs-II-III based on the Ir³⁺-polymers

Each of the series of **NIR-PLEDs-I-III** was fabricated on ITO (Indium tin oxide) coated glass substrates with a sheet resistance of 20 Ω per square. Patterned ITO coated glass substrates were cleaned by a surfactant scrub, washed successively with deionized water, acetone and isopropanol in an ultrasonic bath, and then dried at 120 °C in a heating chamber for 8 h. A 40-nm-thick PEDOT:PSS (Poly(3,4-ethylenedioxythiophene):poly(styrenesulfonate) from water solution was spin-coated (at 2000 rpm) on the substrate and followed by drying in a vacuum oven at 140 °C for 20 min. The chlorobenzene solution (20 mg/mL) of the EML was prepared under an N₂ atmosphere and spin coated (at 4000 rpm) on the PEDOT:PSS layer

with a thickness of 120 nm. The emitting layer difference lies in the usage of PVK:PBD:[Ir(iqbt)₂(vb-ppy)] (65:30:5, wt%) for the NIR-PLED-I, Poly(NVK-co-[Ir(iqbt)₂(vb-ppy)]) (150:1):PBD (70:30, wt%) for the NIR-PLED-II or Poly((vinyl-PBD)-co-NVK-co-[Ir(iqbt)₂(vb-ppy)]) (15:150:1) for the NIR-PLED-III, respectively. Then a hole-blocking layer of TmPyPB (15 nm) were thermally deposited onto the emitting layer. Finally, a thin layer (1 nm) of LiF followed by 100 nm thickness Al capping ayer was deposited onto the substrate under vacuum of 5×10^{-6} Pa. Current density-voltage(*J-V*) characteristics were collected using a Keithley 2400 source meter equipped with acalibrated silicon photodiode. The NIR EL irradiance (*R*) was measured through a PR735 Spectra Scan spectrometer. The eternal quantum efficiencies (η_{EQE}) of the NIR emission were obtained by measuring the irradiance in the forward direction and assuming the eternal emission profile to Lambertian.

References

- 1 J. H. Palmer, A. C. Durrell, Z. Gross, J. R. Winkler and H. B. Gray, *J. Am. Chem. Soc.*, 2010, **132**, 9230-9231.
- 2 G. R. Fu, H. Zheng, Y. N. He, W. T. Li, X.Q. Lü and H. S. He, *J. Mater. Chem. C*, 2018, **6**, 10589-10596.
- 3 S. Kesarkar, W. Mróz, M. Penconi, M. Pasini, S. Destri, M. Cazzaniga, D. Ceresoli, P. R. Mussini, C. Baldoli, U. Giovanella and A. Bossi, *Angew. Chem. Int. Ed.*, 2016, **55**, 2714-2718.
- 4 M. Nonoyama, *Bull. Chem. Soc. Jpn.*, 1979, **52**, 3949-3750.
- 5 Z. Zhang, Y. L. He, L. Liu, X. Q. Lü, X. J. Zhu, W.-K. Wong, M. Pan and C. Y. Su, *Chem.*

- Commun.*, 2016, **52**, 3713-3716.
- 6 J. K. Augustine, V. Vairperrumal, S. Narasimhan, P. Alagarsamy and A. Radhakrishnan, *Tetrahedron*, 2009, **65**, 9989-9996.
- 7 L. Liu, M. Y. Pang, H. T. Chen, G. R. Fu, B. N. Li, X. Q. Lü and L. Wang, *J. Mater. Chem. C*, 2017, **5**, 9021-9027.
- 8 W. R. Wadt and P. J. Hay, *J. Chem. Phys.* 1985, **82**, 284-298.
- 9 P. J. Hay and W. R. Wadt, *J. Chem. Phys.* 1985, **82**, 299-310.
- 10 T. Lu, Multiwfn Manual, version 3.6(dev), Section 3.21.1 and 3.21.8, available at <http://sobereva.com/multiwfn>.
- 11 P. Ros and G. C. A. Schuit, *Theor. Chim. Acta*, 1966, **4**, 44-63.
- 12 T. Lu and F. W. Chen, *J. Comput. Chem.*, 2012, **33**, 580-592.
- 13 Gaussian 09, Revision D.01, M. J. Frisch, G. W. Trucks, H. B. Schlegel, G. E. Scuseria, M. A. Robb, J. R. Cheeseman, G. Scalmani, V. Barone, B. Mennucci, G. A. Petersson, H. Nakatsuji, M. Caricato, X. Li, H. P. Hratchian, A. F. Izmaylov, J. Bloino, G. Zheng, J. L. Sonnenberg, M. Hada, M. Ehara, K. Toyota, R. Fukuda, J. Hasegawa, M. Ishida, T. Nakajima, Y. Honda, O. Kitao, H. Nakai, T. Vreven, J. A. Montgomery, Jr., J. E. Peralta, F. Ogliaro, M. Bearpark, J. J. Heyd, E. Brothers, K. N. Kudin, V. N. Staroverov, R. Kobayashi, J. Normand, K. Raghavachari, A. Rendell, J. C. Burant, S. S. Iyengar, J. Tomasi, M. Cossi, N. Rega, J. M. Millam, M. Klene, J. E. Knox, J. B. Cross, V. Bakken, C. Adamo, J. Jaramillo, R. Gomperts, R. E. Stratmann, O. Yazyev, A. J. Austin, R. Cammi, C. Pomelli, J. W. Ochterski, R. L. Martin, K. Morokuma, V. G. Zakrzewski, G. A. Voth, P. Salvador, J. J. Dannenberg, S. Dapprich, A. D. Daniels, Ö. Farkas, J. B. Foresman, J. V. Ortiz, J. Cioslowski, and D. J. Fox,

Gaussian, Inc., Wallingford CT, 2009.

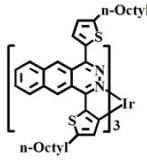
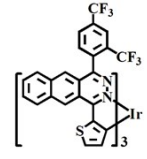
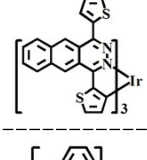
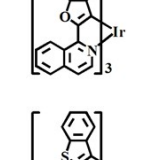
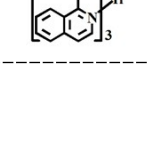
14 H. Y. Chen, C. T. Chen and C. T. Chen, *Macromolecules* 2010, **43**, 3613-3623.

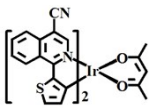
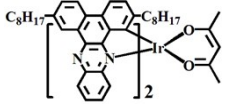
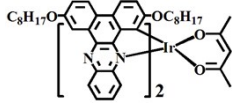
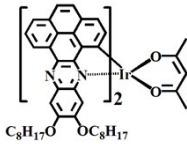
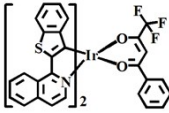
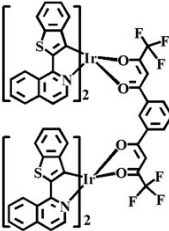
15 E. Zysman-Colman, S. S. Ghosh, G. Xie, S. Varghese, M. Chowdhury, N. Sharma, D. B.

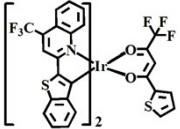
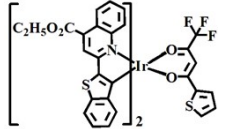
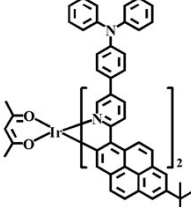
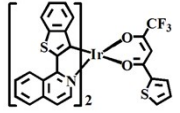
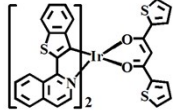
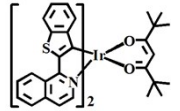
Cordes, A. M. Z. Slawin and I. D. W. Samuel, *ACS Appl. Mater. & Interfaces* 2016, **8**, 9247-

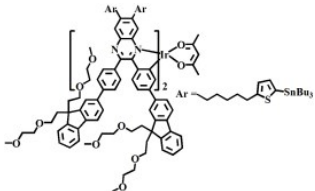
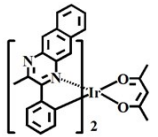
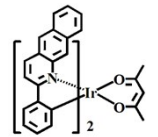
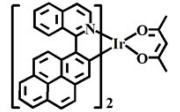
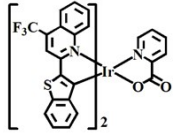
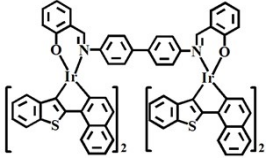
9253.

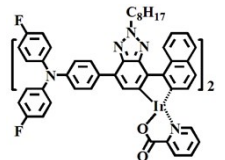
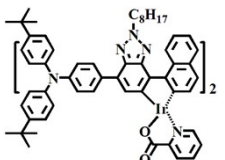
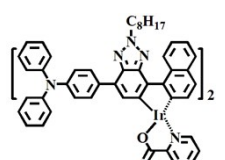
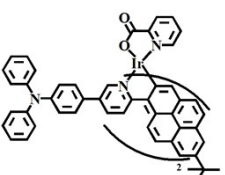
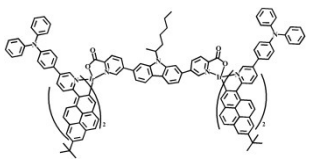
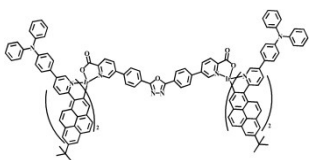
Table S1. The λ_{EL} -relative η_{EQE} summary between the **NIR-PLEDs-I-III** in this work with previously reported Ir(III)-complexes-based vacuum-deposited NIR-OLEDs (NIR-OLEDs-V) and solution NIR-OLEDs (NIR-OLEDs-S) or NIR-PLEDs

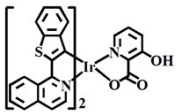
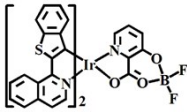
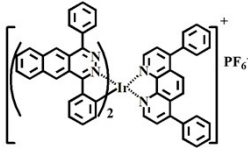
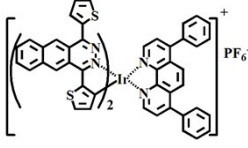
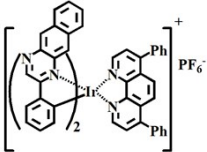
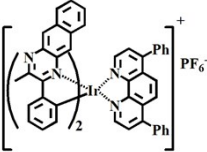
Ir(III)-complex	Chemical structure	Device structure	λ_{EL} (nm)	$\eta_{\text{EQE}}^{\text{max}}$ (%)	Device fabrication	Ref.
Ir(dotbpa) ₃		ITO/PEDOT:PSS/CzTPA-m-Trz: 1 wt% Ir(dotbpa) ₃ /Bphen/LiF/Al	846	0.23	NIR-PLED	6(a)
fac-Ir(Ftbpa) ₃		ITO/NPB/DIC-TRZ:12 wt % fac-Ir(Ftbpa) ₃ /TPBi/Mg:Ag	760	4.50	NIR-OLED-V	6(b)
fac-Ir(dtbp) ₃		ITO/NPB/DIC-TRZ:6 wt % fac-Ir(dtbp) ₃ /TPBi/Mg:Ag	813	0.50	NIR-OLED-V	6(b)
Ir-2a		ITO/PEDOT:PSS/PVCz:PBD:Ir-2a (1.0:0.30:0.04 wt/wt/wt)/CsF/Al	697	0.15	NIR-PLED	6(c)
Ir-2b		ITO/PEDOT:PSS/PVCz:PBD:Ir-2b (1.0:0.30:0.04 wt/wt/wt)/CsF/Al	694	1.41	NIR-PLED	6(c)

Ir(tipCN) ₂ (acac) TCNlr		ITO/HATCN/TAPC/mCP/ TCNlr in CBP (15 wt%)/TPBi/LiF/Al	706	9.59	NIR-OLED-V	7(a)
Ir-R		ITO/PEDOT:PSS/poly-TPD/CBP: Ir-R (1.0 wt%)/TmPyPB/CsF/Al	730	6.91	NIR-OLED-S	7(b)
Ir-OR		ITO/PEDOT:PSS/poly-TPD/PVK:OXD-7(7:3): Ir-OR (0.8 wt%)/TmPyPB/CsF/Al	760	1.45	NIR-PLED	7(b)
(PPZ-11, 12-do) ₂ Ir(acac)		ITO/PEDOT:PSS/poly-TPD/PVK:OXD-7(7:3): (PPZ-11, 12-do)₂Ir(acac) (1 wt%)/TmPyPB/LiF/Al	724	4.14	NIR-PLED	7(c)
[Ir(iqbt) ₂ (btfa)](1)		ITO/PEDOT:PSS/PVK:OXD7: 1 (5 wt%)/LiF/Al	702	1.12	NIR-PLED	7(d)
[(iqbt) ₂ Ir(btp)Ir(iqbt) ₂](2)		ITO/PEDOT:PSS/PVK:OXD7: 2 (5 wt%)/LiF/Al	720	3.11	NIR-PLED	7(d)

(bttmq) ₂ Ir(tta) Ir4		ITO/PEDOT:PSS/mCP:TCTA: Ir4 (10 wt%)/TPBi/Liq/Al	730	0.15	NIR-OLED-S	7(e)
(btecq) ₂ Ir(tta) Ir3		ITO/PEDOT:PSS/mCP:TCTA: Ir3 (10 wt%)/TPBi/Liq/Al	747	0.60	NIR-OLED-S	7(e)
t-BuPyrPyTPA) ₂ Ir(acac)		ITO/PEDOT/PVK:30 wt% OXD-7:4 wt%(t-BuPyrPyTPA) ₂ Ir(acac)/TPBi/Ba/Al	698	0.56	NIR-PLED	7(f)
[Ir(iqbt) ₂ (tta)] (2)		ITO/PEDOT:PSS/PVK(65%):OXD7(30%): 2 (5%)/Ba/Al	709	1.28	NIR-PLED	7(g)
[Ir(iqbt) ₂ (dtdk)] (3)		ITO/PEDOT:PSS/PVK(65%):OXD7(30%): 3 (5%)/Ba/Al	714	2.44	NIR-PLED	7(g)
[Ir(iqbt) ₂ (dpm)](1)		ITO/PEDOT:PSS/PVK(65%):OXD7(30%): 1 (5%)/Ba/Al	714	3.07	NIR-PLED	7(g)

(thdpqx) ₂ Ir(acac)		ITO/PEDOT:PBS/PVK: 40 wt%PBD:(thdpqx) ₂ Ir- (acac) (1%)/TPBi/CsF/Al	704	3.40	NIR-PLED	7(h)
Ir(mpbqx-g) ₂ (acac)(1)		ITO/NPB/complex 1 : Ga ₂ (saph) ₂ Q ₂ (20 wt%)/Bphen/Mg:Ag	780	2.20	NIR-OLED-V	7(i)
Ir(pbq-g) ₂ acac		ITO/NPB/CBP:10% Ir(pbq-g) ₂ acac/Bphen/Mg:Ag	720	1.07	NIR-OLED-V	7(j)
NIR1		ITO/PEDOT/PVK:PBD:NIR15%/LiF/Al	720	0.27	NIR-PLED	7(k)
Ir4		ITO/PEDOT:PSS/PVK/TCTA:PO-T2T:Ir 4 (50:50, 10%)/TPBi /LiF/Al	716	1.08	NIR-OLED-S	8(a)
[(iqbt) ₂ Ir-L ¹ -Ir(iqbt) ₂] (1)		ITO/PEDOT:PSS/PVK:OXD7:1/LiF/Al	710	1.08	NIR-PLED	8(b)

(FTPA-BTz-Iq) ₂ Irpcic		ITO/PEDOT:PSS/PVK/CBP:12 wt%(FTPA-BTz-Iq) ₂ Irpcic/TPBI/Ba/Al	710	0.48	NIR-OLED-S	8(c)
(tBuTPA-BTz-Iq) ₂ Irpcic		ITO/PEDOT:PSS/PVK/CBP:9 wt%(tBuTPA-BTz-Iq) ₂ Irpcic/TPBI/Ba/Al	716	0.66	NIR-OLED-S	8(c)
(TPA-BTz-Iq) ₂ Irpcic		ITO/PEDOT:PSS/PVK/CBP:9 wt%(TPA-BTz-Iq) ₂ Irpcic/TPBI/Ba/Al	712	0.29	NIR-OLED-S	8(c)
Mono-Ir		ITO/PEDOT:PSS/TFB/CBP:PBD: Mono-Ir (60:30:10)/TmPyPB/Liq/Al	698	1.29	NIR-OLED-S	8(d)
D-Ir-Caz		ITO/PEDOT:PSS/TFB/CBP:PBD:D-Ir-Caz(60:30:10)/TmPyPB/Liq/Al	698	0.27	NIR-OLED-S	8(d)
D-Ir-OXD		ITO/PEDOT:PSS/TFB/CBP:PBD:D-Ir-OXD (60:30:10)/TmPyPB/Liq/Al	698	0.41	NIR-OLED-S	8(d)

$[\text{Ir}(\text{iqbt})_2(\text{hpa})](\mathbf{1})$		ITO/PEDOT:PSS/PVK:OXD7:1 (5 wt %)/TmPyPB/LiF/Al	700	2.20	NIR-PLED	8(e)
$[\text{Ir}(\text{iqbt})_2(\text{BF}_2\text{-Hpa})](\mathbf{2})$		ITO/PEDOT:PSS/PVK:OXD7:2 (5 wt %)/LiF/Al	692	0.24	NIR-PLED	8(e)
$[\text{Ir}(\text{dpbpa})_2(\text{Bphen})]^+\text{PF}_6^-$ (1)		ITO/PEDOT:PSS/ PVK:PBD (30 wt%):1 (20 wt%)/TPBI/Cs2CO3/Al	788	0.50	NIR-PLED	9(a)
$[\text{Ir}(\text{dtbpa})_2(\text{Bphen})]^+\text{PF}_6^-$ (2)		ITO/PEDOT:PSS/ PVK:PBD (30 wt%):2 (20 wt%)/TPBI/Cs2CO3/Al	791	0.34	NIR-PLED	9(a)
$[\text{Ir}(\text{pbq-g})_2(\text{Bphen})]^+\text{PF}_6^-$ (1)		ITO/PEDOT:PSS/ PVK:30 wt % PBDorOXD-7:1 (20 wt%)/TPBI/Cs2CO3/zAl (120 nm)	693	0.67	NIR-PLED	9(b)
$[\text{Ir}(\text{mpbqx-g})_2(\text{Bphen})]^+\text{PF}_6^-$ (2)		ITO/PEDOT:PSS/PVK:30 wt % PBDorOXD-7:2 (20 wt%)/TPBI/Cs2CO3/zAl	753	0.61	NIR-PLED	9(b)

[Ir(iqbt) ₂ (vb-ppy)]		ITO/PEDOT:PSS/ PVK:PBD:[Ir(iqbt) ₂ (vb-ppy)]/TmPyPB/LiF/Al	696	4.12	NIR-PLED-1	This work
Poly(NVK-co-[Ir(iqbt) ₂ (vb-ppy)])		ITO/PEDOT:PSS/ Poly(NVK-co-[Ir(iqbt) ₂ (vb-ppy)])(150:1):PBD/TmPyPB/LiF/Al	692	2.45	NIR-PLED-II	This work
Poly((vinyl-PBD)-co-NVK-co-[Ir(iqbt) ₂ (vb-ppy)])		ITO/PEDOT:PSS/ Poly((vinyl-PBD)-co-NVK-co-[Ir(iqbt) ₂ (vb-ppy)])(15:150:1)/TmPyPB/LiF/Al	694	3.56	NIR-PLED-III	This work

Table S2. Photo-physical properties of the ligands **Hiqbt**, **vb-Hppy** and **vinyl-PBD**, the complex monomer **[Ir(iqbt)₂(vb-ppy)]** in degassed CH₂Cl₂ solution and its grafting-type Ir³⁺-polymers **Poly(NVK-co-[Ir(iqbt)₂(vb-ppy)])** (100:1, 150:1 or 200:1) and **Poly((vinyl-PBD)-co-NVK-co-[Ir(iqbt)₂(vb-ppy)])** (15:150:1) in solid-state at RT or 77 K

complex	Absorption ^[a]	Emission (RT) ^{[a]/[b]}			Emission (77 K) ^[a]		Energy level ^[c,d]		Thermal properties
	λ_{abs}	λ_{em}	τ	Φ_{m}	λ_{em}	τ	HOMO	LUMO	$\Delta T_{5\%}/T_{\text{g}}$
	[nm]	[nm]	[μs]		[nm]	[μs]	(eV)	(eV)	(°C)
Hiqbt	312, 344	415 ^[a]	-	-	?	?	?	?	?
vb-Hppy	307	403 ^[a]	-	-	?	?	?	?	?
vinyl-PBD	318	421 ^[a]	-	-	?	?	?	?	?
[Ir(iqbt)₂(vb-ppy)]	292, 318, 430, 456, 524, 663	^[a] 693, 754(sh)	0.25	0.19	704, 764(sh)	0.38	-5.17 (-4.68)	-3.03 (-1.88)	384
Poly(NVK-co-[Ir(iqbt)₂(vb-ppy)])									
(100:1)	228, 261, 293, 329, 342	698 ^[b]	0.97	0.13	?	?	-5.25	-3.10	407/164
(150:1)	228, 261, 293, 329, 343	696 ^[b]	1.24	0.16	?	?	-5.23	-3.08	405/162
(200:1)	228, 261, 293, 330, 343	690 ^[b]	1.29	0.21	?	?	-5.21	-3.03	403/161
Poly((vinyl-PBD)-co-NVK-co-[Ir(iqbt)₂(vb-ppy)])									
(15:150:1)	228, 261, 293, 330, 343	693 ^[b]	1.25	0.17	?	?	-5.29	-3.19	408/187

^[a]In degassed CH₂Cl₂ solution; ^[b]in solid-state; ^[c,d]HOMO and LUMO levels are obtained from electrochemical determination and theoretical calculation, respectively.

Table S3. TD-DFT calculation results for the complex monomer **[Ir(iqbt)₂(vb-ppy)]** based on the optimized S₀ states.

Complex	Contribution of d _π and π orbitals of ligands to MOs (%)					Main configuration of S ₀ → S _n excitation, λ _{cal} (nm)/f ^a	Main configuration of S ₀ → T _n excitation, λ _{cal} (nm) ^b

	Orbital	Ir	iqbt-1	iqbt-2	vb-ppy		
[Ir(iqbt)₂(vb-ppy)]	LUMO+2	2.83	8.33	1.91	86.93	S ₀ → S ₁ : H → L (97.64), 557.5, 0.0415	S ₀ → T ₁ : H-1 → L (30.32%); H → L (59.94%), H → L+1 (3.56%), 694.7
	LUMO+1	3.68	84.71	1.48	10.22	S ₀ → S ₂ : H → L+1 (95.32), 512.3, 0.0788	S ₀ → T ₂ : H-1 → L (2.06%); H-1 → L+1 (10.13%); H → L+1 (73.77%); H → L+2 (4.91%), 676.7
	LUMO	4.33	0.33	92.76	2.58	S ₀ → S ₃ : H → L+2 (97.26), 488.9, 0.0073	S ₀ → T ₃ : H-1 → L (48.60%); H → L (34.52%), 529.6
	HOMO	23.73	51.01	23.06	2.20		
	HOMO-1	1.24	31.75	66.04	0.97	S ₀ → S ₄ : H-2 → L (13.54), H-1 → L 76.73), H → L (5.45), 444.7, 0.0057	
	HOMO-2	14.59	17.42	57.02	10.97		

^aH → L denotes the transition from HOMO to LUMO. λ_{cal}, and f denote the calculated emission wavelength, and oscillator strength, respectively.

^bThe oscillator strength of S₀ → T₁ is zero owing to the spin-forbidden character of the singlet-triplet transition under TD-DFT calculations in the Gaussian program with no consideration of spin orbital coupling.

Table S4. NTO results for the complex monomer **[Ir(iqbt)₂(vb-ppy)]** based on the optimized T₁ states.

Complex	Contribution of d _π and π orbitals of ligands to NTOs (%)				
	NTO	Ir	iqbt-1	iqbt-2	vb-ppy
[Ir(iqbt)₂(vb-ppy)]	Partical	5.70	0.10	92.58	0.74
	Hole	12.35	2.56	82.25	0.44

Table S5. GPC data of the grafting-type Ir³⁺-polymers **Poly(NVK-co-[Ir(iqbt)₂(vb-ppy)])** (100:1, 150:1 or 200:1) and **Poly((vinyl-PBD)-co-NVK-co-[Ir(iqbt)₂(vb-ppy)])** (15:150:1)

Sample	NVK/monomer	<i>M_n</i> /(g/mol)	PDI
Poly(NVK-co-[Ir(iqbt)₂(vb-ppy)])	100:1	7003	1.26
	150:1	9769	1.28
	200:1	12111	1.27
Poly((vinyl-PBD)-co-NVK-co-[Ir(iqbt)₂(vb-ppy)])	15:150:1	14693	1.30

Figure S1. ^1H NMR spectra for the ligands **Hiqbt**, **vb-Hppy** and **vinyl-PBD**, the vinyl-functionalized complex monomer **$[\text{Ir}(\text{iqbt})_2(\text{vb-ppy})]$** and its two series of grafting-type Ir^{3+} -polymers **$\text{Poly}(\text{NVK-co-}[\text{Ir}(\text{iqbt})_2(\text{vb-ppy})])$** (150:1) and **$\text{Poly}((\text{vinyl-PBD})\text{-co-NVK-co-}[\text{Ir}(\text{iqbt})_2(\text{vb-ppy})])$** (15:150:1) in $\text{DMSO-}d_6$ or CDCl_3 at RT.

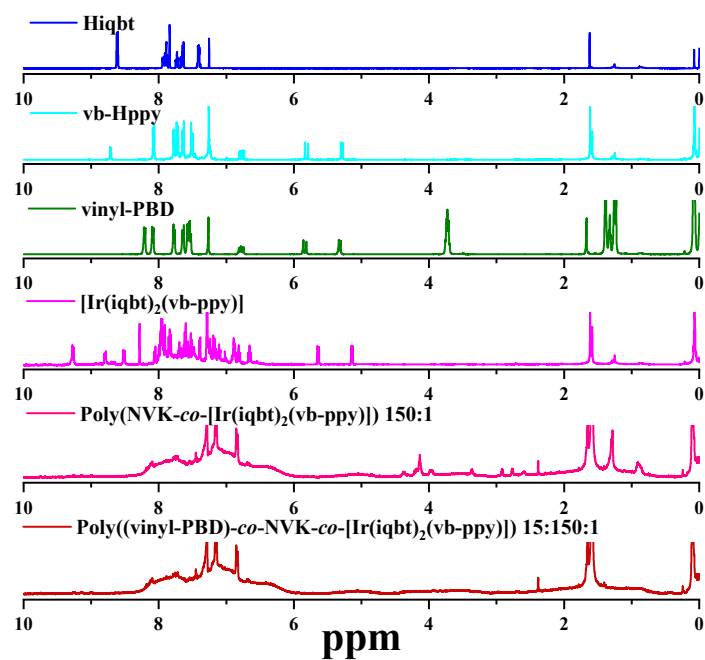


Figure S2 Normalized UV-visible absorption and emission spectra for the ligands **Hiqbt**, **vb-Hppy** and **vinyl-PBD** in degassed CH_2Cl_2 solution at RT.

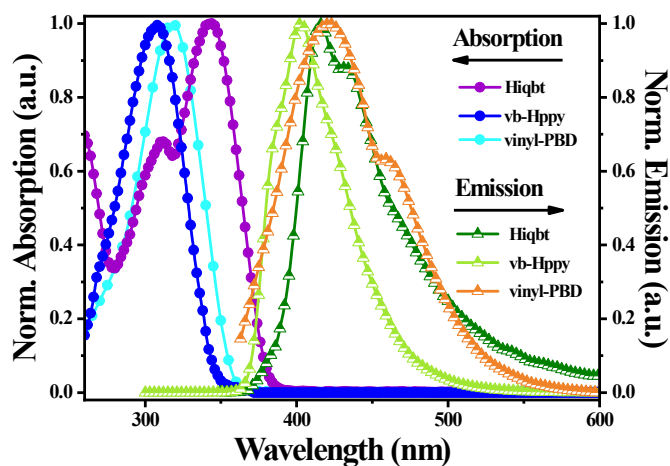


Figure S3. The mono-exponential time-decayed ($\lambda_{em} = 693$ nm) curve of the complex monomer **[Ir(iqbt)₂(vb-ppy)]** in degassed CH₂Cl₂ solution at RT.

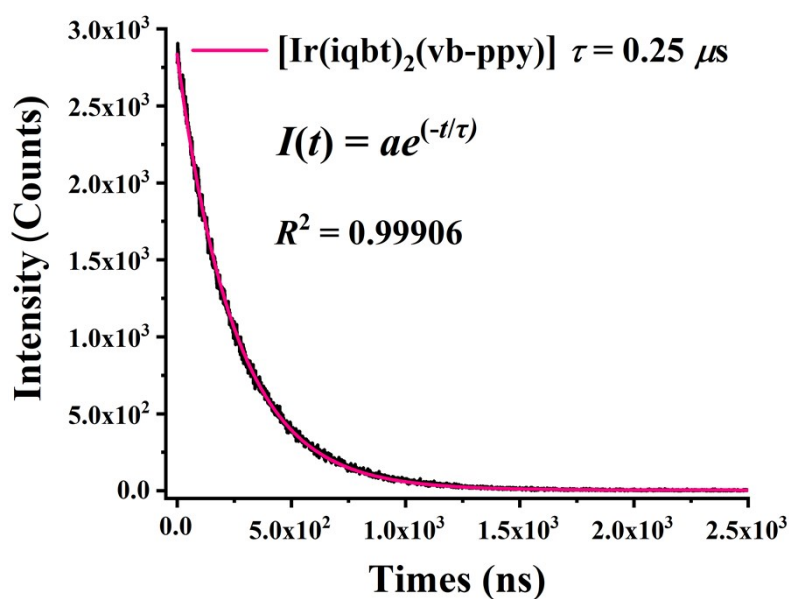


Figure S4. The TG and DSC (inset) curves of the complex monomer **[Ir(iqbt)₂(vb-ppy)]** and the grafting-type Ir³⁺-polymers **Poly(NVK-co-[Ir(iqbt)₂(vb-ppy)])** (100:1, 150:1 or 200:1) and **Poly((vinyl-PBD)-co-NVK-co-[Ir(iqbt)₂(vb-ppy)])** (15:150:1) in solid state.

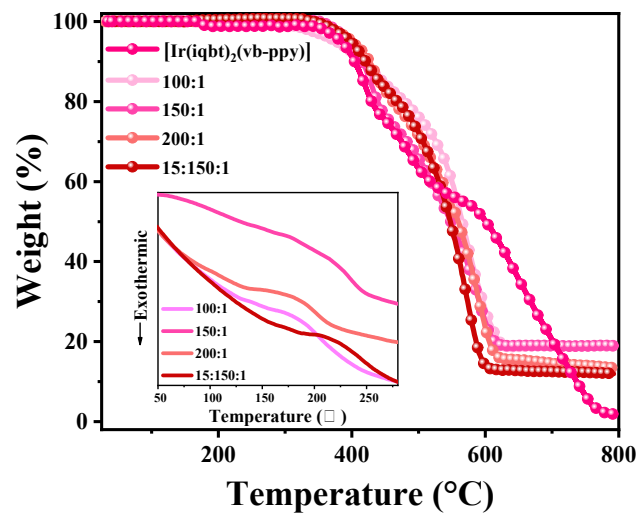


Figure S5. PXRD patterns of the grafting-type Ir³⁺-polymers **Poly(NVK-co-[Ir(iqbt)₂(vb-ppy)])** (100:1, 150:1 or 200:1) and **Poly((vinyl-PBD)-co-NVK-co-[Ir(iqbt)₂(vb-ppy)])** (15:150:1) in solid-state at RT.

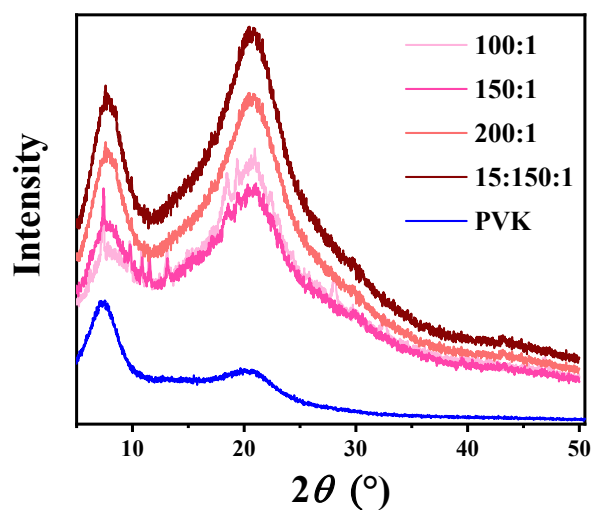


Figure S6. Normalized DR (down) and UV-visible-NIR absorption (up) spectra of the grafting-type Ir³⁺-polymers **Poly(NVK-co-[Ir(iqbt)₂(vb-ppy)])** (100:1, 150:1 or 200:1) and **Poly(vinyl-PBD)-co-NVK-co-[Ir(iqbt)₂(vb-ppy)]** (15:150:1) in solid state or solution at RT.

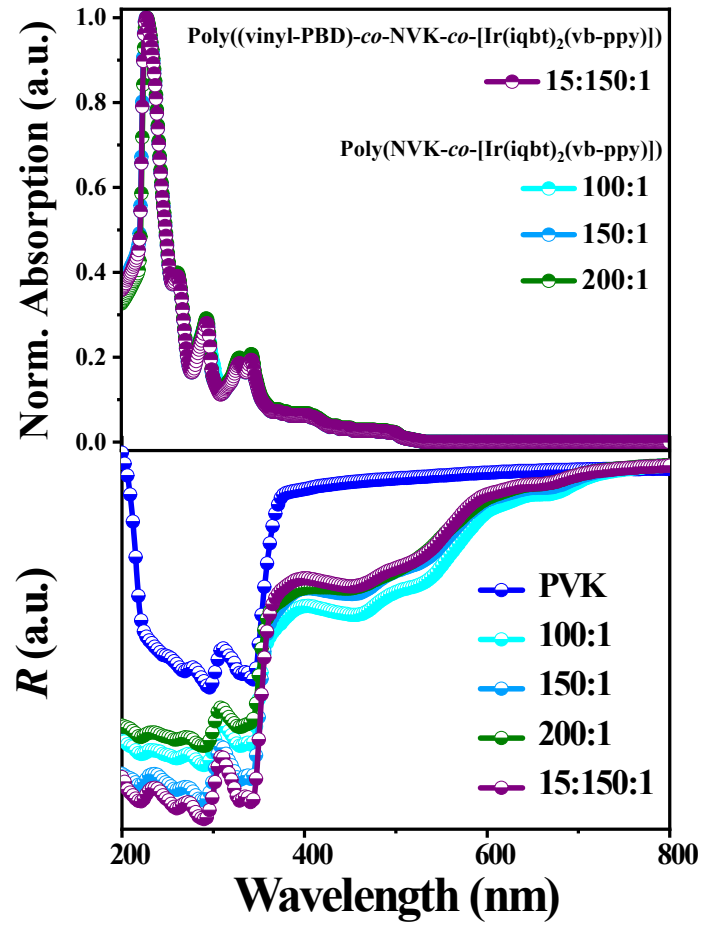


Figure S7. The mono-exponential time-decayed ($\lambda_{em} = 690\text{-}696\text{ nm}$) curves of the grafting-type Ir^{3+} -polymers **Poly(NVK-co-[Ir(iqbt)₂(vb-ppy)])** (100:1, 150:1 or 200:1) and the bipolar Ir^{3+} -polymer **Poly((vinyl-PBD)-co-NVK-co-[Ir(iqbt)₂(vb-ppy)])** (15:150:1) in solid state at RT.

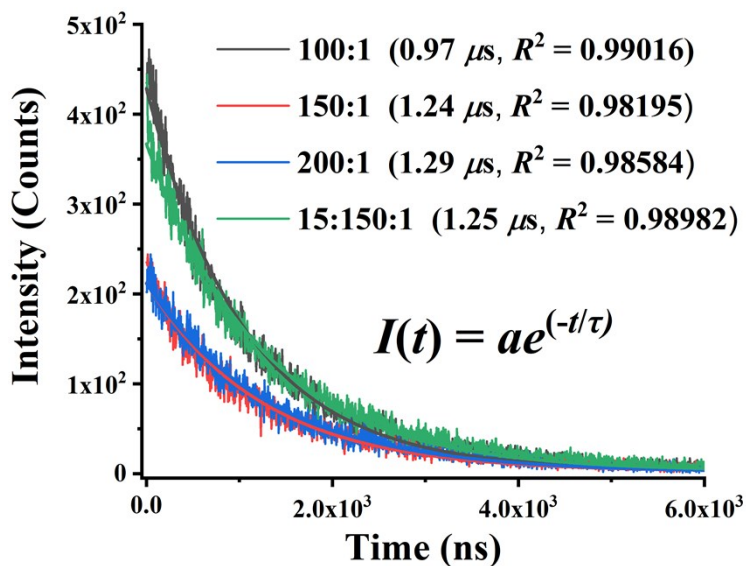


Figure S8. Cyclic voltammogram (CV) curve for the complex monomer **[Ir(iqbt)₂(vb-ppy)]** in HPLC-grade CH_3CN solution at RT under a N_2 atmosphere (scan rate = 100 mV s^{-1}).

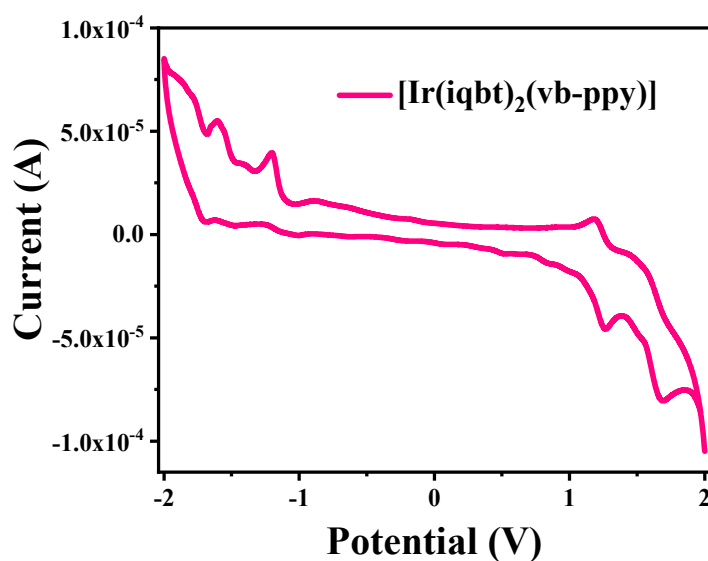


Figure S9. CV curves for the grafting-type Ir^{3+} -polymers **Poly(NVK-co-[Ir(iqbt)₂(vb-ppy)])**

(100:1, 150:1 or 200:1) and **Poly((vinyl-PBD)-co-NVK-co-[Ir(iqbt)₂(vb-ppy)])** (15:150:1) in

HPLC-grade CH₂Cl₂ solution at RT under a N₂ atmosphere (scan rate = 100 mV s⁻¹).

